Glucose-induced phosphatidylinositol 3-kinase and mitogen-activated protein kinase-dependent upregulation of the platelet-derived growth factor-B receptor potentiates vascular smooth muscle cell chemotaxis

Published in:
Diabetes

Glucose-Induced Phosphatidylinositol 3-Kinase and Mitogen-Activated Protein Kinase–Dependent Upregulation of the Platelet-Derived Growth Factor-β Receptor Potentiates Vascular Smooth Muscle Cell Chemotaxis

Malcolm Campbell,[1] William E. Allen,[1] Jonathan A. Silversides,[1] and Elisabeth R. Trimble[1,2]

The aim of this study was to investigate the effects of elevated D-glucose concentrations on vascular smooth muscle cell (VSMC) expression of the platelet-derived growth factor (PDGF)β receptor and VSMC migratory behavior. Immunoprecipitation, immunofluorescent staining, and RT-PCR of human VSMCs showed that elevated D-glucose induced an increase in the PDGFβ receptor that was inhibited by phosphatidylinositol 3-kinase (PI3K) and mitogen-activated protein kinase (MAPK) pathway inhibitors. Exposure to 25 mmol/l D-glucose (HG) induced increased phosphorylation of protein kinase B (PKB) and extracellular-regulated kinase (ERK). All HG chemotaxis assays (with either 10 days' preincubation in HG or no preincubation) in a FCS or PDGF-BB gradient showed positive chemotaxis, whereas those in 5 mmol/l D-glucose did not. Assays were also run with concentrations ranging from 5 to 25 mmol/l D-glucose. Chemotaxis was induced at concentrations ≥9 mmol/l D-glucose. An anti-PDGFβ receptor antibody inhibited glucose-potentiated VSMC chemotaxis, as did the inhibitors for the PI3K and MAPK pathways. This study has shown that small increases in D-glucose concentration, for a short period, increase VSMC expression of the PDGFβ receptor and VSMC sensitivity to chemotactic factors in serum, leading to altered migratory behavior in vitro. It is probable that similar processes occur in vivo with glucose-enhanced chemotaxis of VSMCs, operating through PDGFβ receptor–operated pathways, contributing to the accelerated formation of atheroma in diabetes. *Diabetes* 52: 519–526, 2003

Vascular disease is responsible for much of the excess morbidity and mortality that affect patients with diabetes. The atherosclerotic plaque contains components derived from both the endothelial and muscle layers in addition to invading macrophages (1,2), as is the case for all causes of atheroma formation. However, clinically significant atherosclerosis occurs at an earlier age and is often more severe in patients who suffer from diabetes than in nondiabetic subjects (1).

Platelet-derived growth factor (PDGF), secreted by vascular cells, plays a central role in the development of atherosclerotic proliferation of vascular smooth muscle cells (VSMCs) (2). PDGF also stimulates chemotaxis (3). The effects of PDGF are mediated through binding to specific high-affinity surface receptors (4). Since PDGF receptors are found on VSMCs (5) and macrophages (6), this suggests that PDGF could influence atherosclerosis by regulating the functions of both macrophages and VSMCs.

Macrophages are present at all stages of development of the atherosclerotic plaque. Macrophages adhere to endothelial cells, move between these cells, and accumulate in the subendothelial space (7). Activated macrophages not only act as scavenger cells but also secrete several growth factors. Secretions of growth factors such as PDGF (8) and colony-stimulating factor (CSF)-1 (9) are increased when macrophages are activated. Glucose causes an upregulation of the CSF-1 receptor (*c-fms*) on macrophages (10), thereby allowing enhanced autocrine activation of the macrophage by CSF-1.

A high glucose environment causes the development of oxidative stress within VSMCs (11,12), and both this and/or the presence of increased amounts of chemotactic substances cause VSMCs to change their phenotype and migrate into the subendothelial space. VSMCs in the subendothelial space display a "secretory" phenotype expressing genes for a number of growth factors and their receptors such as *c-fms* (2). A range of factors, such as urokinase type plasminogen activator (13), thrombospondin-1 (14), bone morphogenetic protein-2 (BMP-2) (15), tumor necrosis factor-α (16), vascular endothelial growth factor (17), and IGF-1 (18), are believed to be

chemotactic for VSMCs. At present, PDGF is the best-characterized chemotactic agent for VSMCs (19).

The aims of this study were to determine whether high glucose levels per se induce alterations in the expression of the PDGFβ receptor in primary human aortic VSMCs, to determine the signaling pathways involved, and to determine whether the chemotactic properties of VSMCs are altered by exposure to high glucose. High glucose concentrations cause VSMCs to divide. In this study, the movement of cells has been investigated using a Dunn chamber, which allows dividing and nondividing cells to be identified and treated separately. This assay is also more sensitive than the more commonly used transwell assay (20,21). Additionally, it allows accurate calculation of the speed of cell movement, which cannot be assessed in the transwell assay.

RESEARCH DESIGN AND METHODS

Chemicals and antibodies. D-Glucose and L-glucose were purchased from BDH (Poole, UK). PDGF-BB was purchased from Insight Biotechnology (Wembly, UK). Wortmannin and LY294002 were purchased from Sigma (Poole, UK). PD-98059 was from Calbiochem (La Jolla, CA). Trolox and α-lopoic acid were from Sigma.

The following antibodies were used: anti-PDGFβ receptor and anti-PDGFα receptor antibodies (R&D Systems, Minneapolis, MN), rabbit polyclonal antibody to total extracellular-regulated kinase (ERK) (Santa Cruz), mouse polyclonal antibody to phosphorylated ERK (Santa Cruz), rabbit polyclonal antibody to Akt/protein kinase B (PKB) phosphorylated on serine 473 (Cell Signaling Technology), rabbit polyclonal antibody against Akt/PKB (Cell Signaling Technology), and horseradish peroxidase (HRP)-conjugated donkey anti-mouse IgG and HRP-conjugated donkey anti-rabbit IgG (Dako, Ely, UK).
Isolation of VSMCs. Porcine aorta was obtained from the local abattoir. VSMCs were isolated and grown as previously described (11,12). Human VSMCs were obtained from the thoracic aorta of transplant donors (written consent was obtained from the relevant family member, and the study was approved by the Ethical Committee of Queen's University, Belfast). The VSMCs were isolated as previously described (11,12), except that the growth medium was RPMI-1640 (GibcoBRL, Life Technologies, Paisley, UK) instead of Dulbecco's modified Eagle's medium (GibcoBRL). Cells were confirmed as VSMCs by positive immunofluorescence staining with a monoclonal antibody against smooth muscle α-actin. All VSMC experiments were carried out using cells of passage 4–7.
Chemotaxis assays. Chemotaxis was assessed by direct observation and recording of cell behavior in stable concentration gradients of FCS using the Dunn chemotaxis chamber (Weber Scientific International, Teddington, UK). This apparatus permits the direction of migration of individual cells to be measured in relation to the direction of the gradient, as well as the time course of the response to be followed (20–22). The chamber was set up, filmed, and the data analyzed as previously described (20–22). In FCS gradient experiments, FCS-free medium was placed in the inner well and 10% FCS medium in the outer well. For PDGF-BB gradient experiments, cells were serum starved for 4 h before the Dunn chamber was assembled. In these experiments, the medium in the outer well was replaced with serum-free medium containing 10 ng/ml PDGF-BB (Insight Biotechnology). Experiments were run for 18 h with a time-lapse interval of 10 min. To test for chemotaxis, the Rayleigh test for unimodal clustering of directions was applied to the data and a *P* value of <0.01 was chosen as the criterion for rejecting the null hypothesis of random directionality (23). Where there was significant unimodal clustering, the mean direction and its 95% CI were calculated. The Student's *t* test was used to compare migration speeds between experiments.

This assay was used to test a range of glucose conditions and the following pharmacological agents: wortmannin (10 nmol/l) and LY294002 (10 μmol/l) (phosphatidylinositol 3-kinase [PI3K] inhibitors), PD-98059 (10 μmol/l) (a mitogen-activated protein kinase [MAPK] inhibitor), and blocking antibodies against the PDGFα and -β receptors.
Immunofluorescence. For immunofluorescence studies, cells were fixed in 4% formaldehyde in PBS for 20 min at room temperature and then permeabilized with 0.5% Triton X-100 in PBS containing 1% BSA for 10 min. Actin filaments were stained by incubation with 0.1 mg/ml tetramethyl rhodamine isothiocyanate (TRITC)-labeled phalloidin (Sigma Chemical) for 60 min. For localization of the PDGFβ receptor, cells were incubated for 60 min at room temperature with a 1:200 dilution of goat anti-PDGFβ receptor (R&D Systems)

in a PBS/1% BSA blocking buffer before incubation for 60 min with 1:100 fluorescein isothiocyanate-conjugated mouse anti-goat IgG (Caltag) in blocking buffer. Staining for the PDGFα receptor was carried out as for the PDGFβ receptor, with the substitution of the PDGFα receptor antibody.
Immunoprecipitation. Adherent cells were washed with ice-cold PBS, incubated in RIPA buffer on ice for 20 min before being scraped, and left on ice for 60 min. Cell lysate was centrifuged at 10,000 rpm for 10 min. Mouse IgG1 (0.25 μg) (Dako) and 20 μl protein A-G Plus Agarose (Santa Cruz) were added to lysate containing 200 μg protein for each condition and incubated at 4°C for 30 min. The supernatant was removed to fresh tubes after centrifugation at 2,500 rpm for 5 min. Mouse anti-PDGFβ receptor (5 μl), rabbit anti-ERK (5 μl) (Santa Cruz), mouse anti-pERK (5 μl) (Santa Cruz), rabbit anti-pPKB (Cell Signaling Technology), or rabbit anti-PKB (Cell Signaling Technology) was added to the supernatant and incubated at 4°C for 1 h. Protein A-G Plus Agarose (20 μl) was added to the mixture and incubated overnight at 4°C. The mixture was then pelleted by centrifugation at 2,500 rpm for 5 min. The pellet was washed four times with ice-cold RIPA buffer. After the final wash, the pellet was resuspended in 40 μl of Laemli buffer. For Western blotting, proteins were resolved in 4–20% Tris HCl gels and transferred to nitrocellulose membrane at 200 mA for 2 h (Amersham Pharmacia Biotech, Buckinghamshire, UK). Membranes were blocked with PBS/5% fat-free dried milk/0.1% Tween 20. For detection, rabbit anti-ERK (Santa Cruz), mouse anti-pERK (Santa Cruz), rabbit anti-pPKB (Cell Signaling Technology), rabbit anti-PKB (Cell Signaling Technology), or mouse anti-PDGFβ receptor (R&D Systems) were used at a dilution of 1:500. Detection was with HRP-conjugated donkey anti-rabbit IgG (Dako) or HRP-conjugated donkey anti-mouse IgG (Dako) at 1:1,000 and enhanced chemiluminescence (Supersignal Ultra; Pierce, Rockford, IL). UK Analysis of results was carried out by densitometry (GS-670 Imaging densitometer; Bio-Rad Laboratories).
RT-PCR. Total RNA was extracted using a RNeasy midi kit (Qiagen) before one-step RT-PCR using a Reverse-It One-Step kit (ABgene, Epsom, UK). Briefly, 1 μg RNA was added to ReddyMix RT-PCR master mix containing 0.2 μmol/l sense/antisense primers (PDGFβ forward primer corresponds to nucleotides 2,805–2,824 and PDGFβ reverse primer to nucleotides 3,317–3,300 of the PDGFβ cDNA) (24), 1.25 units Thermoprime Plus DNA polymerase, 0.2 mm dNTP mix, 1.5 mm MgCl₂, and 2.5 units Reverse-It Blend. The reactions were subjected to the following cycling conditions: first-strand synthesis (47°C for 30 min), RTase inactivation and initial denaturation (94°C for 2 min followed by 30 cycles of denaturation 94°C for 20 s), annealing (50°C for 30 s), and extension (72°C for 1 min); final extension was performed at 72°C for 5 min. Target mRNA was coamplified with the internal control (GAPDH), which acted as a control for sample-to-sample variation in RT and PCR and monitored the extent of degradation and recovery of RNA. PCR were separated using 1.2% Agarose gel before visualization and quantification using Gene Tools analysis software (Snygene, Poole, Dorset, UK).

RESULTS

Glucose induces increased growth factor receptor expression in VSMCs. To determine the effect of exposure to elevated D-glucose, immunofluorescent staining, immunoprecipitation, and RT-PCR were carried out for the PDGFβ receptor.

Confocal laser microscopy demonstrated that human VSMCs express the PDGFβ receptor (Fig. 1*A* and *B*). Comparison of the cells cultured in 5 mmol/l (Fig. 1*A*) and 25 mmol/l D-glucose (Fig. 1*B*) suggested that the PDGFβ receptors were increased in 25 mmol/l D-glucose; quantitative image analysis revealed a 110% increase compared with 5 mmol/l D-glucose in staining for the PDGFβ receptor in 25 mmol/l D-glucose. Immunofluorescent staining also demonstrated that human VSMCs express the PDGFα receptor; however, no change in expression was detected between 5 and 25 mmol/l D-glucose (data not shown).

Western blotting of human and porcine VSMC-immunoprecipitated lysates was carried out to gain a more quantitative comparison of the expression of the PDGFβ receptor between 5 and 25 mmol/l glucose. Densitometry showed that VSMCs exposed to 25 mmol/l D-glucose for 1 day had a 60% increase in the PDGFβ receptor compared with 5 mmol/l (Fig. 1*C*), whereas VSMCs exposed to 25
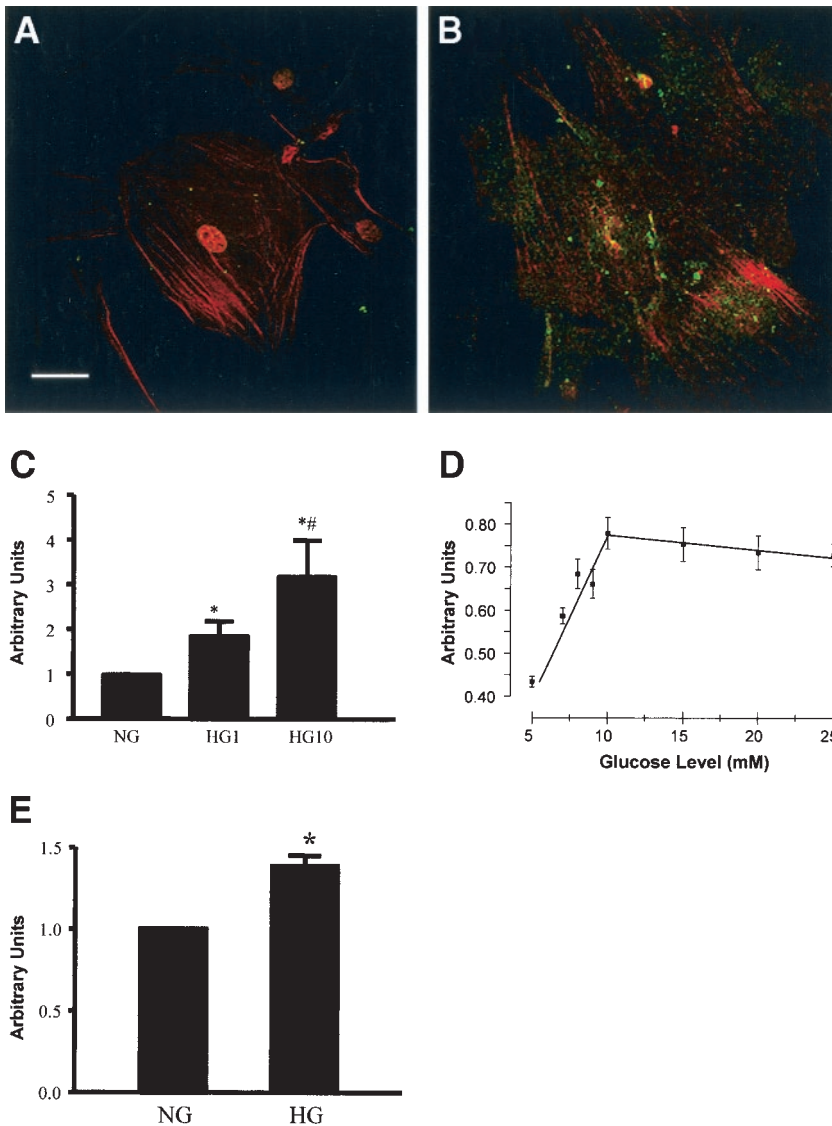
FIG. 1. Expression of PDGFβ receptors on VSMCs. Human VSMCs were stained for the PDGFβ receptor in conditions of 5 (*A*) or 25 mmol/l glucose (*B*) for 24 h. Cells were stained for the receptors (green) and f-actin (red). This receptor was expressed, and present in greater quantity, in cells exposed to 25 mmol/l glucose (quantitative image analysis indicates a 110% increase). Scale bar represents 10 μm. Immunoprecipitation and Western blotting of VSMCs revealed that after a 1-day exposure to 25 mmol/l D-glucose (HG1), VSMCs show a 60% increase, and that after a 10-day exposure to 25 mmol/l glucose (HG10), show a 214% increase in PDGFβ receptor when compared with 5 mmol/l glucose (NG) ($n = 6$) (*C*). Quantitative image analysis of VSMCs exposed to concentrations of glucose ranging from 5 to 25 mmol/l and stained for PDGFβ receptor showed that expression of this receptor increases with increasing glucose concentration up to 10 mmol/l glucose. Above this concentration, receptor expression plateaus ($n = 3$) (*D*). RT-PCR showed that 24 h exposure to 25 mmol/l glucose significantly increased PDGFβ receptor mRNA ($n = 14$). *$P < 0.05$ vs. NG; #$P < 0.05$ vs. HG1.

mmol/l D-glucose for 10 days showed a 214% increase in the PDGFβ receptor compared with 5 mmol/l D-glucose.

To determine how high the glucose concentration needed to be to cause an increase in PDGFβ receptor expression, VSMCs exposed to a range of glucose concentrations from 5 to 25 mmol/l for 24 h were stained. Quantitative image analysis showed that with increasing glucose concentration up to 10 mmol/l, PDGFβ receptor expression increased before leveling off at concentrations between 10 and 25 mmol/l (Fig. 1*D*).

RT-PCR showed that 24 h exposure to 25 mmol/l glucose induced a significant increase in PDGFβ receptor mRNA (Fig. 1*E*).

Glucose induces increased PDGF receptor expression via PI3K and MAPK pathways. Pharmacological agents were used to determine which major second messenger systems regulate glucose-induced increases in PDGFβ receptor expression. VSMCs were placed in 25 mmol/l glucose in the presence of standard concentrations of wortmannin (10 nmol/l), LY294002 (10 μmol/l) (PI3K inhibitors), or PD-98059 (10 μmol/l) (MAPK inhibitor) for 24 h. Immunoprecipitation and RT-PCR were carried out for the PDGFβ receptor. Treatment with wortmannin or

LY294002 led to significant reduction of the PDGFβ receptor protein, as did treatment with PD-98059 (Fig. 2*A*). These agents were dissolved in DMSO, necessitating a DMSO control. To determine whether this inhibition effect was specific to the effects of high glucose, LY294002 and PD-98059 were also tested in 5-mmol/l glucose conditions. In 5 mmol/l glucose, both LY294002 and PD-98059 caused a slight reduction in expression of the receptor. RT-PCR showed that both LY294002 and PD-98059 cause significant inhibition of the PDGFβ receptor mRNA levels compared with the 25 mmol/l glucose/DMSO control (Fig. 2*B*).

These results indicate that the glucose-induced upregulation of the PDGFβ receptor is PI3K and MAPK dependent and that there is a low level of PI3K and MAPK pathway activity in 5 mmol/l D-glucose.

Glucose leads to increased phosphorylation of PKB and ERK. The effects of glucose on the PI3K pathway was assessed by investigation of protein kinase B (PKB or Akt) a downstream target for PI3K. Immunoprecipitation was carried out for total PKB and phosphorylated PKB. Densitometry revealed that levels of total PKB were not altered by exposure to 25 mmol/l glucose (Fig. 3*A*), but that after 24 h exposure to 25 mmol/l glucose, there was an increase
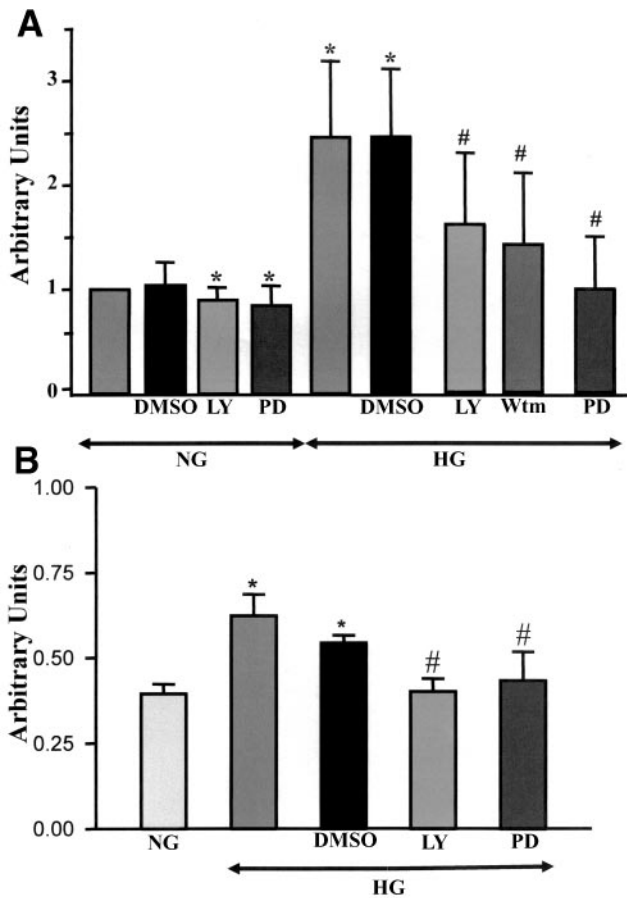
FIG. 2. Effects of PI3K and MAPK inhibitors on PDGFβ receptor expression. Immunoprecipitation and Western blotting of VSMCs revealed that after 24 h exposure to 25 mmol/l D-glucose (HG) and treatment with the PI3K inhibitors wortmannin (10 nmol/l) (Wtm) or LY294002 (10 μmol/l) (LY), or the MAPK inhibitor PD-98059 (10 μmol/l) (PD), the expression of the PDGFβ receptor was significantly reduced compared with the HG DMSO control (*n* = 5) (*A*). RT-PCR of VSMCs also revealed that after 24 h exposure to HG and treatment with LY294002 or PD-98059, the mRNA levels for the PDGFβ receptor were significantly reduced compared with the HG DMSO control (*n* = 4) (*B*). *$P < 0.05$ vs. 5 mmol/l glucose; #$P < 0.05$ vs. HG/DMSO.
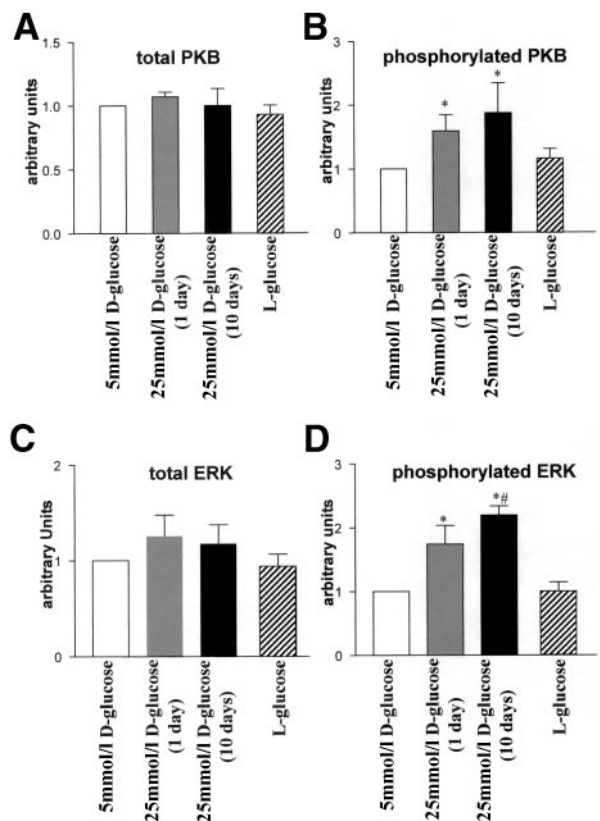

FIG. 3. Effects of high glucose concentration on PKB and ERK phosphorylation. Immunoprecipitation and densitometry showed that exposure to 25 mmol/l D-glucose had no significant effect on the expression of total PKB after either 1 or 10 days. Ten days' exposure to 5 mmol/l D-glucose and 20 mmol/l L-glucose (osmotic and glycation control) had no significant effect on total PKB expression (*A*). High D-glucose exposure for 1 day increased the levels of PKB phosphorylation, which increased further with 10 days' exposure; however, 10 days' exposure to 5 mmol/l D-glucose and 20 mmol/l L-glucose had no significant effect on PKB phosphorylation (*B*). Immunoprecipitation and densitometry showed that exposure to 25 mmol/l D-glucose or 5 mmol/l D-glucose and 20 mmol/l L-glucose had no significant effect on the expression of total ERK 1/2 after either 1 or 10 days (10 days only for L-glucose) (*C*). Exposure to 25 mmol/l glucose for both 1 and 10 days significantly increased the level of ERK 1/2 phosphorylation, but 10 days' exposure to 5 mmol/l D-glucose plus 20 mmol/l L-glucose did not (*D*) (*n* = 8). *$P < 0.05$ vs. 5 mmol/l glucose; # $P < 0.05$ vs. 25 mmol/l glucose for 1 day.

of phosphorylated PKB compared with 5 mmol/l glucose (Fig. 3*B*), and that after 10 days' exposure to 25 mmol/l glucose, the levels of phosphorylated PKB were further increased (Fig. 3*B*). Exposure to 5 mmol/l D-glucose plus 20 mmol/l L-glucose had no effect on either total PKB expression or the amount of phosphorylated PKB.

To further investigate the role of the MAPK pathway, immunoprecipitation was carried out for total ERK 1/2 (Fig. 3*C*) and phosphorylated ERK 1/2 (Fig. 3*D*). No significant increase in the expression of ERK 1/2 was detected (Fig. 3*C*); however, measurement of phosphorylated ERK showed a significant increase in ERK 1/2 phosphorylation after 24-h exposure to 25 mmol/l glucose, which increased further after 10 days' exposure (Fig. 3*D*). Exposure to 5 mmol/l D-glucose plus 20 mmol/l L-glucose had no effect on either total ERK 1/2 expression or the amount of phosphorylated ERK 1/2.

To address the possibility that the changes in PKB and ERK activity was caused by increased oxidative stress, PKB and ERK were measured in cells exposed to the antioxidants α-lipoic acid (50 μmol/l) and Trolox (200

μmol/l) in 25 mmol/l D-glucose. No effect was noted (data not shown).

Glucose sensitizes VSMCs to PDGF and serum factors. To test the effects of increased glucose concentrations on human VSMC migration, cells were exposed to a gradient of FCS in either 5 or 25 mmol/l D-glucose using the Dunn chemotaxis chamber. The 25 mmol/l D-glucose–treated cells had been preincubated in 25 mmol/l D-glucose for 10 days before the experiment. In 5 mmol/l D-glucose, the human VSMCs moved randomly (Fig. 4*A*). By contrast, in 25 mmol/l D-glucose, the cells showed chemotaxis toward the source of the FCS (Fig. 4*B*). This experiment was repeated using porcine VSMCs; again in 5 mmol/l D-glucose, the cells moved randomly in the FCS gradient but chemotaxed in 25 mmol/l D-glucose (data not shown).

To test whether a 10-day exposure to 25 mmol/l D-glucose was required to induce this alteration in behavior, human VSMCs cultured in 5 mmol/l D-glucose were exposed to 25 mmol/l D-glucose only when placed in the

$n = 33, P = 0.240$ $n = 34, P < 0.001$ $n = 36, P < 0.001$

$n = 33, P < 0.001$ $n = 32, P < 0.001$ $n = 37, P < 0.001$

$n = 35, P = 0.302$ $n = 30, P = 0.245$ $n = 32, P < 0.001$

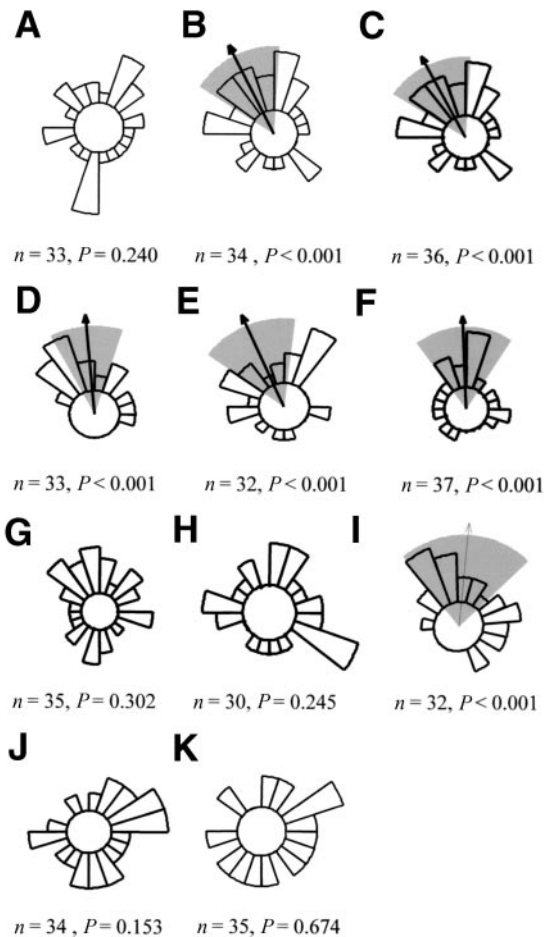$n = 34, P = 0.153$ $n = 35, P = 0.674$

FIG. 4. VSMC migration in a gradient of FCS. Circular histograms show the proportion of human VSMCs migrating in each direction, with the source of FCS at the top. The Rayleigh test showed that cells exposed to 5 mmol/l glucose (*A*) did not show chemotaxis, while those exposed to 25 mmol/l D-glucose for 10 days did show chemotaxis to FCS (*B*). Human VSMCs exposed to 25 mmol/l D-glucose, only when placed within the Dunn chamber without a prior 10-day incubation, also showed chemotaxis (*C*), as did those exposed to 15 (*D*), 10 (*E*), and 9 (*F*) mmol/l glucose. However, human VSMCs exposed to 8 mmol/l glucose did not show chemotaxis to FCS (*G*). Human VSMCs exposed to 25 mmol/l D-glucose and preincubated for 5 h with a neutralizing anti-PDGFβ receptor antibody did not show chemotaxis in a gradient of FCS (*H*). Human VSMCs exposed to 25 mmol/l D-glucose and preincubated for 5 h with a neutralizing anti-PDGFα receptor antibody showed chemotaxis in a gradient of FCS (*I*). Human VSMCs exposed to 5 mmol/l D-glucose and 20 mmol/l L-glucose for 10 days did not show chemotaxis to FCS (*J*). Human VSMCs exposed to 25 mmol/l glucose (no 10-day preincubation) in isotonic FCS (with 10% FCS in both the source and sink well) move randomly (*K*). All experiments were run for 18 h; *n* represents the number of cells tracked, and *P* represents Rayleigh test probability. All graphs represent the combined results of at least four independent experiments.

chemotaxis chamber. As with the 10-day preincubation experiments, the cells showed chemotaxis (Fig. 4*C*).

Intermediate concentrations of D-glucose were tested. It was shown that in 15, 10, and 9 mmol/l D-glucose (without preincubation), there was chemotaxis (Fig. 4*D*, *E*, and *F*, respectively). However, in 8 mmol/l D-glucose, there was no chemotaxis (Fig. 4*G*). Because PDGF is known to be a chemotactic agent for VSMCs and because high glucose upregulates the PDGFβ receptor (Fig. 1), human VSMCs were preincubated for 5 h with either an antibody against the PDGFβ receptor (1 μg/ml) or the PDGFα receptor (1 μmg/ml) in 25 mmol/l D-glucose before being exposed to a gradient of FCS, in order to determine whether PDGF

$n = 33, P = 0.240$ $n = 34, P < 0.001$
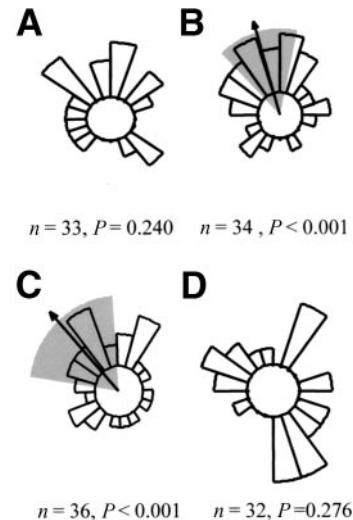
$n = 36, P < 0.001$ $n = 32, P = 0.276$

FIG. 5. VSMC migration in a gradient of PDGF-BB. Circular histograms show the proportion of cells migrating in each direction, with the source of PDGF-BB at the top. The Rayleigh test showed that cells exposed to 5 mmol/l D-glucose and 10 ng/ml PDGF-BB (*A*) did not show chemotaxis, whereas those exposed to 25 mmol/l D-glucose and 10 ng/ml PDGF-BB within the Dunn chamber did show chemotaxis (*B*). Human VSMCs exposed to 5 mmol/l D-glucose in a stronger gradient (30 ng/ml) of PDGF-BB showed chemotaxis (*C*). Human VSMCs exposed to 25 mmol/l D-glucose preincubated for 5 h with a neutralizing anti-PDGFβ receptor antibody did not show chemotaxis in a gradient of PDGF-BB (*D*). All assays were run for 18 h; *n* represents the number of cells tracked, and *P* represents Rayleigh test probability. All graphs represent the combined results of at least four independent experiments.

plays a role in the chemotaxis to FCS in high glucose concentrations. The PDGFβ receptor antibody blocked chemotaxis in the FCS gradient (Fig. 4*H*); however, the PDGFα receptor antibody did not inhibit chemotaxis (Fig. 4*I*). Incubation with a nonrelevant IgG of the same species and class had no effect on chemotaxis (data not shown). This indicated that PDGF within the FCS played a key role in producing the chemotaxis shown in Fig. 4*B*. Control experiments were carried out to eliminate the possibility that the change in migratory behavior was caused by either osmosis or glycation. To achieve this, human VSMCs were exposed to 5 mmol/l D-glucose plus 20 mmol/l L-glucose for 10 days and did not show chemotaxis (Fig. 4*J*). A second control was carried out to eliminate the possibility that some characteristic of the Dunn chemotaxis chamber influenced the change in VSMC behavior. In these experiments, human VSMCs in 25 mmol/l D-glucose were placed in the chamber with 10% FCS in both the source and sink well, i.e., FCS throughout the chamber; in the absence of an FCS gradient, there was no chemotaxis (Fig. 4*K*).

The effects of glucose on PDGF-induced chemotaxis were tested. Human VSMCs were maintained in RPMI without FCS for 4 h before being placed in a gradient of PDGF-BB (10 ng/ml) in either 5 or 25 mmol/l D-glucose. No chemotaxis occurred in 5 mmol/l D-glucose (Fig. 5*A*), whereas it did occur in 25 mmol/l D-glucose (Fig. 5*B*). A very high concentration of PDGF-BB (30 ng/ml) did induce chemotaxis in 5 mmol/l glucose (Fig. 5*C*). If cells were preincubated with the anti-PDGFβ receptor antibody before being placed in a gradient of PDGF-BB in 25 mmol/l D-glucose, no chemotaxis was observed (Fig. 5*D*). Again, as a control, cells were also incubated with a nonrelevant
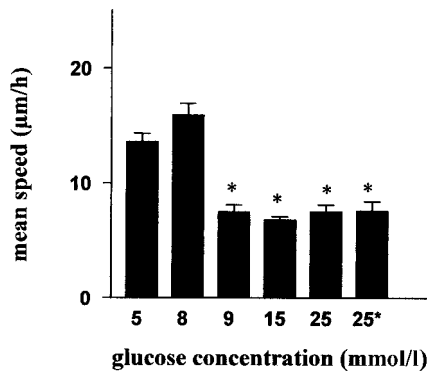
FIG. 6. Speed of movement. Bar graph showing the mean speeds (and standard errors) of human VSMCs exposed to various glucose concentrations within the Dunn chamber, in a gradient of FCS. Speed of cell movement was significantly reduced in glucose concentrations ≥ 9 mmol/l (i.e., in all concentrations of glucose in which chemotaxis to FCS occurs). 25*, cells exposed to 25 mmol/l D-glucose for 10 days (all other cells were maintained in 5 mmol/l glucose before the experiment). *$P < 0.05$ vs. 5 mmol/l glucose.

IgG of the same species and class that had no effect on chemotaxis (data not shown).

Analysis of the speed of cell movement showed a significant drop in cell speed, at 9 mmol/l glucose and higher, in gradients of FCS (Fig. 6).

Glucose-potentiated chemotaxis is PI3K and MAPK dependent. VSMCs were placed in a gradient of FCS in 25 mmol/l glucose in the presence of 10 nmol/l wortmannin or 10 µmol/l LY294002 or PD-98059. The cells were exposed to each inhibitor within the chamber, and the experiments were carried out in a darkened room due to the light sensitivity of these inhibitors. It was found that the cells treated with the inhibitors wortmannin (Fig. 7A), LY294002 (Fig. 7B), and PD-98059 (Fig. 7C) did not show chemotaxis in the FCS gradient. As these agents are
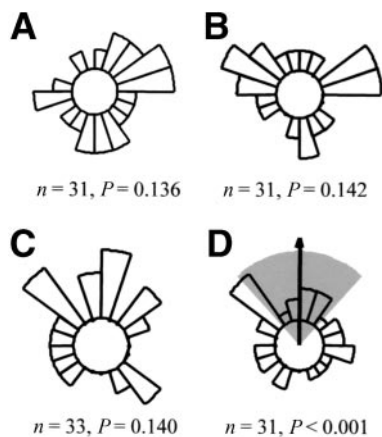

FIG. 7. Glucose-potentiated VSMC chemotaxis is PI3K and MAPK dependent. Circular histograms show the proportion of human VSMCs migrating in each direction, with the source of FCS at the top. The Rayleigh test showed that cells exposed to 25 mmol/l glucose and incubated in 10 nmol/l wortmannin (a PI3K inhibitor) failed to show chemotaxis (A), as did those exposed to 25 mmol/l glucose and the 10 µmol/l LY294002 (another PI3K inhibitor) (B). The Rayleigh test also showed that cells treated with 10 µmol/l PD-98059, a MAPK inhibitor (C), and exposed to 25 mmol/l D-glucose do not show chemotaxis. A control experiment was run with cells exposed to 25 mmol/l glucose and DMSO (as wortmannin, LY294002 and PD-98059 are soluble in DMSO), which showed chemotaxis (D). All experiments were run for 18 h; n represents the number of cells tracked, and P represents Rayleigh test probability. Graphs show the combined results of three to four independent experiments.

soluble in DMSO, a control experiment was run with 1 µl/ml DMSO present in 25 mmol/l glucose, and the cells in this experiment showed positive chemotaxis (Fig. 7D). Treatment with each of these inhibitors significantly reduced the speed of the cells compared with untreated cells in 25 mmol/l glucose (data not shown). These results indicate that the D-glucose–potentiated chemotaxis in the FCS gradient was mediated via PI3K and MAPK.

Glucose induces increased f-actin and filopodia formation in VSMCs. The actin cytoskeleton is a major component of the cellular migratory apparatus (25). Porcine VSMCs were fixed and stained using TRITC-conjugated phalloidin and then visualized using a confocal laser-scanning microscope. This clearly showed an increase in the amount of f-actin within the VSMCs exposed to 25 mmol/l D-glucose compared with 5 mmol/l D-glucose (Fig. 8A and B).

Staining of sparsely plated porcine VSMCs allowed the peripheral actin structures, lamellipodia and filopodia, to be observed. Lamellipodia are broad sheet-like structures (Fig. 8C, arrow), while filopodia (also known as microspikes) are fine spike-like actin structures (25). The number of filopodia (Fig. 8D, arrows) was increased in 25 mmol/l glucose (Fig. 8D) compared with 5 mmol/l glucose (Fig. 8C). This finding is consistent with the chemotaxis results, as filopodia have been shown to be essential for chemotaxis (25).

DISCUSSION

Because PDGF is suspected to play a central role in the proliferation and migration of VSMCs in atherosclerosis (2,3,26), the aim of this study was to investigate in detail the effects of exposure to elevated glucose concentrations of primary human aortic VSMCs on the expression of the PDGF receptors and how this altered expression affects chemotaxis of human aortic VSMCs. The study also aimed to determine whether PI3K- and MAPK-mediated pathways play a role in glucose-induced altered expression of the PDGF receptors.

Results obtained by immunofluorescent staining and immunoprecipitation showed that in high glucose, the expression of the PDGFβ receptor is increased. RT-PCR showed an increase in PDGFβ receptor mRNA, indicating that glucose alters transcription of the gene.

Treatment with inhibitors to PI3K and MAPK showed that glucose-induced upregulation of the PDGFβ receptor is dependent on both the PI3K and MAPK pathways. This is further supported by the finding that 25 mmol/l glucose induced an increase in phosphorylation of both PKB (PI3K pathway) and ERK (MAPK pathway). In light of the fact that previous studies found that glucose-induced PDGFβ receptor expression was protein kinase C dependent (6,27), these findings indicate that the mechanisms by which high glucose alters PDGFβ receptor expression are complex.

Results obtained in this study demonstrated that raised concentrations of glucose were able to increase the sensitivity of VSMCs to serum factors and PDGF-BB, inducing chemotaxis in a gradient of FCS. It may seem surprising that in 5 mmol/l D-glucose, VSMCs do not show chemotaxis to FCS or PDGF-BB. Many cells will show chemotaxis in a gradient of FCS (regardless of glucose
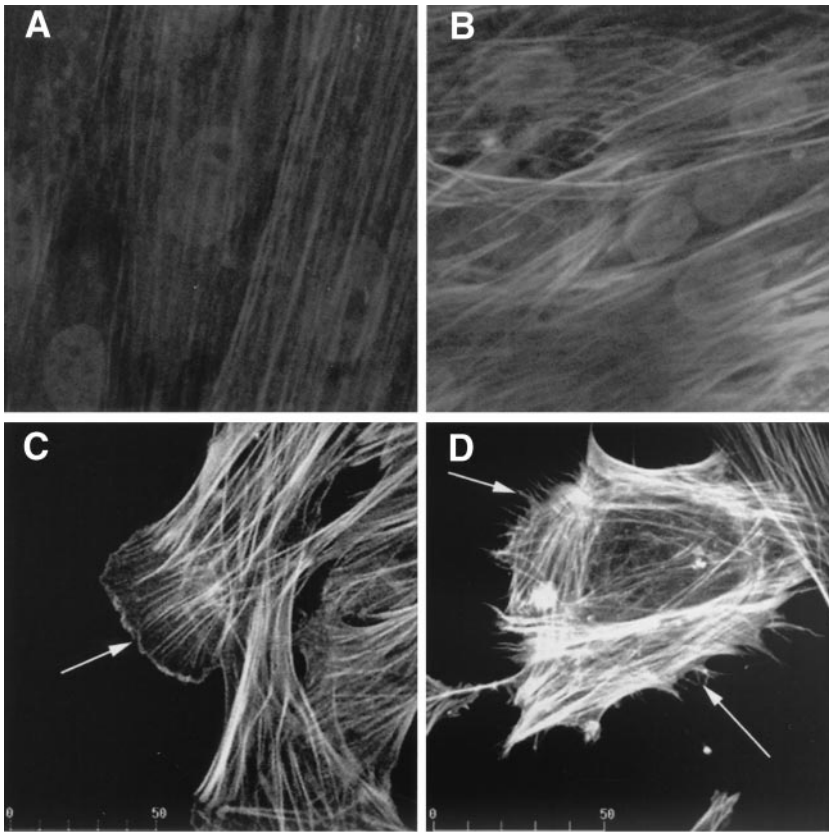
FIG. 8. The VSMC actin cytoskeleton. Porcine VSMCs were exposed to either 5 or 25 mmol/l glucose for 24 h, fixed, and stained with TRITC-conjugated phalloidin to allow visualization of the actin cytoskeleton. These stained cells were imaged using a confocal laser-scanning microscope. In the cells exposed to 25 mmol/l glucose (B), the TRITC staining was markedly more intense than in cells exposed to 5 mmol/l glucose (A); because the staining protocol and all settings on the microscope were identical, this indicates an increase in the amount of f-actin present. Examination of the peripheral actin cytoskeleton revealed that in 25 mmol/l glucose (D), more filopodia (arrows in D) are present than in 5 mmol/l glucose (C). No apparent difference in lamellipodia (arrow in C) number or distribution was noticed. Scale bars represent 50 μm.

concentration) if cultured in the absence of FCS for an extended period of time (which upregulates receptor expression); however, without this serum starvation, most cells will not respond to a gradient of FCS. Increasing the concentration of PDGF-BB to 30 ng/ml induced chemotaxis in 5 mmol/l glucose.

The change in chemotactic behavior occurred after short periods of exposure to relatively modest increases in the concentration of glucose. This was an interesting finding in light of the high-glucose–induced increase in PDGFβ receptors. It is possible that this upregulation of receptors could explain the greater sensitivity of VSMCs to FCS and PDGF-BB in high glucose than in normal glucose; this conclusion was supported by the observation that treatment with an antibody against the PDGFβ receptor prevented human VSMC chemotaxing in either the FCS or PDGF-BB gradients. Use of both PI3K and MAPK pathway inhibitors blocked glucose-potentiated VSMC chemotaxis, again showing the importance of these pathways in glucose-modified VSMC biology.

Morphological examination of the actin cytoskeleton showed both an increase in total f-actin and an increase in the number of filopodia in VSMCs exposed to raised concentrations of glucose. This is an interesting finding since it has been previously shown that filopodia play a crucial role in macrophage chemotaxis (25).

Glucose has been shown to directly stimulate cell migration in a human umbilical vein endothelial cell (HUVEC)-derived cell line (24). By contrast, high glucose concentrations have been shown to inhibit neural crest cell migration in rat embryos (28). It is also possible that other high-glucose–induced processes, such as polyol accumulation (29), nonenzymatic glycation of proteins (29–

32), and altered redox potential (33), mediate this change in migratory behavior. Yasunari et al. (34), who preincubated cells in high glucose for 72 h, found that the aldose reductase inhibitor epalrestat did inhibit glucose potentiated VSMC chemotaxis to PDGF, suggesting a role for the polyol pathway. However, it is well established that in high glucose, it requires 2–3 days for the subsequent increase in diacylglycerol levels to rise in VSMCs (35–37); therefore, since the chemotatic behavior shown in the present study occurred without prior incubation in high glucose, it is unlikely that it is mediated by this mechanism. The receptor for advanced glycation end products has been shown to mediate rabbit smooth muscle cell chemotaxis (38). In the present study, chemotaxis occurred without prior incubation in glucose but did not occur when cells were incubated for 10 days with L-glucose, which, although not metabolized, can cause glycation. This suggests that advanced glycation end product–related phenomena were not responsible for the chemotactic behavior of VSMCs in high glucose seen in the present study.

It is perhaps surprising that in the present study, the speed of cell movement was significantly lower in concentrations of glucose that potentiate chemotaxis to FCS, i.e., 9 mmol/l D-glucose and higher. In macrophages, inhibition of Cdc42, which leads to loss of chemotaxis to CSF-1, also causes an increase in the speed of cell movement (25), suggesting that movement by chemotaxis is slower than random movement.

In conclusion, the results presented above show that exposure to even modest and short-lived increases in glucose concentration potentiate VSMC chemotaxis to serum factors by inducing an upregulation of PDGF receptors and possibly other growth factor receptors by PI3K

and MAPK signaling pathway–dependent processes. Taken together with our earlier finding that exposure to high glucose concentrations increases VSMC proliferation (11,12), these findings provide the cellular basis for one of the many mechanisms that contribute to atherosclerosis in diabetes.

REFERENCES

1. McVeigh GE, Brennan GM, Johnston GD, McDermott BJ, McGrath LT, Henry WR, Andrews JW, Hayes JR: Impaired endothelium-dependent and independent vasodilation in patients with type 2 (non-insulin-dependent) diabetes mellitus. *Diabetologia* 35:771–776, 1992
2. Ross R: The pathogenesis of atherosclerosis: a perspective for the 1990s. *Nature* 362:801–809, 1993
3. Williams LT: Signal transduction by the platelet-derived growth factor receptor. *Science* 243:1564–1570, 1989
4. Frackelton AJ, Tremble PM, Williams LT: Evidence for the platelet-derived growth factor-stimulated tyrosine phosphorylation of the platelet-derived growth factor receptor in vivo: immunopurification using a monoclonal antibody to phosphotyrosine. *J Biol Chem* 259:7909–7915, 1984
5. Feuerstein GZ, Ruffolo RR Jr: Carvedilol, a novel multiple action antihypertensive agent with antioxidant activity and the potential for myocardial and vascular protection. *Eur Heart J* 16 (Suppl. F):38–42, 1995
6. Inaba T, Ishibashi S, Gotoda T, Kawamura M, Morino N, Nojima Y, Kawakami M, Yazaki Y, Yamada N: Enhanced expression of platelet-derived growth factor-β receptor by high glucose: involvement of platelet-derived growth factor in diabetic angiopathy. *Diabetes* 45:507–512, 1996
7. O'Brien SF, Watts GF, Playford DA, Burke V, O'Neal DN, Best JD: Low-density lipoprotein size and high density lipoprotein concentration, and endothelial dysfunction in non insulin dependent diabetes. *Diabet Med* 114:974–978, 1997
8. Hughes AD, Clunn GF, Refson J, Demoliou-Mason C: Platelet-derived growth factor (PDGF): actions and mechanisms in vascular smooth muscle. *Gen Pharmacol* 27:1079–1089, 1996
9. Abordo EA, Westwood ME, Thornalley PJ: Synthesis and secretion of M-CSF by mature human monocytes and human monocytic THP-1 cells induced by human serum albumin derivatives modified with methylglyoxal and glucose-derived advanced glycation end products. *Immunol Lett* 53:7–13, 1996
10. Saini A, Liu YJ, Cohen DJ, Ooi BS: Hyperglycemia augments macrophage growth responses to colony-stimulating factor-1. *Metabolism* 45:1125–1129, 1996
11. Sharpe PC, Yue KKM, Catherwood MA, McMaster D, Trimble ER: The effects of glucose-induced oxidative stress on growth and extracellular matrix gene expression of vascular smooth muscle cells. *Diabetologia* 41:1210–1219, 1998
12. Sharpe PC, Liu W-H, Yue KKM, McMaster D, Catherwood MA, McGinty AM, Trimble ER: Glucose-induced oxidative stress in vascular contractile cells: comparison of aortic smooth muscle cells with retinal pericytes. *Diabetes* 47:801–809, 1998
13. Lymn JS, Rao SJ, Clunn GF, Gallagher KL, O'Neill C, Thompson NT, Mardia KV: *Statistics of Directional Data*. London, Academic Press, 1972
14. Gahtan V, Wang XJ, Willis AI, Tuszynski GP, Sumpio BE: Thrombospondin-1 regulation of smooth muscle cell chemotaxis is extracellular signal-regulated protein kinases 1/2 dependent. *Surgery* 128:203–207, 1999
15. Willette RN, Gu JL, Lysko PG, Anderson KM, Minehart H, Yue T: BMP-2 gene expression and effects on human vascular smooth muscle cells. *J Vasc Res* 36:120–125, 1999
16. Goetze S, Xi XP, Kawano Y, Kawano H, Fleck E, Hsueh WA, Law RE: TNF-alpha-induced migration of vascular smooth muscle cells is MAPK dependent. *Hypertension* 33:183–189, 1999
17. Wang H, Keiser JA: Vascular endothelial growth factor upregulates the expression of matrix metalloproteinases in vascular smooth muscle cells: role of flt-1. *Circ Res* 83:832–840, 1998
18. Cospedal R, Abedi H, Zachary I: Platelet-derived growth factor-BB regulation of migration and focal adhesion kinase phosphorylation in rabbit aortic vascular smooth muscle cells: roles of phosphatidylinositol 3-kinase and mitogen-activated protein kinases. *Cardiovasc Res* 41:708–721, 1999
19. Doanes AM, Irani K, Goldschmidt-Chermont PJ, Finkel T: A requirement for rac1 in the PDGF-stimulated migration of fibroblasts and vascular smooth cells. *Biochem Mol Biol Int* 45:279–287, 1998
20. Zicha D, Dunn GA, Brown AF: A new direct-viewing chemotaxis chamber. *J Cell Sci* 99:769–775, 1991
21. Zicha D, Dunn GA, Jones GE: Analyzing chemotaxis using the direct-viewing chamber. In *Basic Cell Culture Protocols*. Pollard JW, Walker JM, Eds. Totowa, NJ, Humana Press, 1997, p. 449–458
22. Vanhaesebroeck B, Jones GE, Allen WE, Zicha D, Hooshmand-Rad R, Sawyer C, Wells C, Waterfield MD, Ridley AJ: Distinct PI 3Ks mediate mitogenic signalling and cell migration in macrophages. *Nature Cell Biol* 1:69–71, 1999
23. Dunn GA, Zicha D: Dynamics of fibroblast spreading. *J Cell Sci* 108:1239–1249, 1992
24. Shigematsu S, Yamauchi K, Nakajima K, Iijima S, Aizawa T, Hashizume K: D-glucose and insulin stimulate migration and tubular formation of human endothelial cells in vitro. *Am J Physiol* 277:E433–E438, 1999
25. Allen WE, Zicha D, Ridley AJ, Jones GE: A role for Cdc42 in macrophage chemotaxis. *J Cell Biol* 141:1147–1157, 1998
26. Ross R, Glomset JA: The pathogenesis of atherosclerosis. *N Engl J Med* 295:369–377, 1976
27. Nakamura J, Kasuya Y, Hamada Y, Nakashima E, Naruse K, Yasuda Y, Kato K, Hotta N: Glucose-induced hyperproliferation of cultured rat aortic smooth muscle cells through polyol pathway hyperactivity. *Diabetologia* 44:480–487, 2001
28. Suzuki N, Svensson K, Eriksson UJ: High glucose concentration inhibits migration of rat cranial neural crest cells in vitro. *Diabetologia* 39:401–411, 1996
29. Kikkawa R, Umemura K, Haneda M, Kajiwara N, Maeda S, Nishimura C, Shigeta Y: Identification and characterization of aldose reductase in cultured rat mesangial cells. *Diabetes* 41:1165–1171, 1992
30. Hammes HP, Wellensiek B, Kloting I, Sickel E, Bretzel RG: The relationship of glycaemic level to advanced glycation end-product (AGE) accumulation and retinal pathology in the spontaneous diabetic hamster. *Diabetologia* 41:165–170, 1998
31. Hasegawa G, Hunter AJ, Charonis AS: Matrix nonenzymatic glycosylation leads to altered cellular phenotype and intracellular tyrosine phosphorylation. *J Biol Chem* 270:3278–3283, 1995
32. Wautier JL, Wautier MP, Schmidt AM, Anderson GM, Hori O, Zoukourian C, Capron L, Chappey O, Yan SD, Brett J, Guillausseau PJ, Stern D: Advanced glycation end products (AGEs) on the surface of diabetic erythrocyte bind to the vessel wall via a specific receptor inducing oxidant stress in the vasculature: a link between surface-associated AGEs and diabetic complications. *Proc Natl Acad Sci U S A* 91:7742–7746, 1994
33. Williamson JR, Chang K, Frangos M, Hasan KS, Ido Y, Kawamura T, Nyengaard JR, van den Enden M, Kilo C, Tilton RG: Hyperglycemic pseudohypoxia and diabetic complications. *Diabetes* 42:801–813, 1993
34. Yasunari K, Kohno M, Kano H, Minami M, Yoshikawa J: Aldose reductase inhibitor improves insulin-mediated glucose uptake and prevents migration of human coronary artery smooth muscle cells induced by high glucose. *Hypertension* 35:1092–1098, 2000
35. Shiba T, Inoguchi T, Sportsman JR, Heath WF, Bursell S, King GL: Correlation of diacylglycerol level and protein kinase C activity in rat retina to retinal circulation. *Am J Physiol* 265:E783–E793, 1993
36. Xia P, Inoguchi T, Kern TS, Engerman RL, Oates PJ, King GL: Characterization of the mechanism for the chronic activation of diacylglycerol-protein kinase C pathway in diabetes and hypergalactosemia. *Diabetes* 43:1122–1129, 1994
37. Inoguchi T, Xia P, Kunisaki M, Higashi S, Feener EP, King GL: Insulins's effect on protein kinase C and diacylglycerol induced by diabetes and glucose in vascular tissues. *Am J Physiol* 267:E369–E379, 1994
38. Higashi T, Sano H, Saishoji T, Ikeda K, Jinnouchi Y, Kanzaki T, Morisaki N, Rauvala H, Shichiri M, Horiuchi S: The receptor for advanced glycation end products mediates the chemotaxis of rabbit smooth muscle cells. *Diabetes* 46:463–472, 1997